Journal of Applied Physics

RESEARCH ARTICLE | DECEMBER 26 2012

Application of non-metal doped titania for inverted polymer solar cells

Katarzyna Siuzdak; Mamatimin Abbas; Laurence Vignau; Mélanie Devynck; Galina V. Dubacheva; Anna Lisowska-Oleksiak

J. Appl. Phys. 112, 123110 (2012)
https://doi.org/10.1063/1.4770490

AIP Publishing

Application of non-metal doped titania for inverted polymer solar cells

Katarzyna Siuzdak,[1,2,3] Mamatimin Abbas,[2,a)] Laurence Vignau,[2] Mélanie Devynck,[2] Galina V. Dubacheva,[4] and Anna Lisowska-Oleksiak[1]
[1]*Department of Chemical Technology, Chemical Faculty, Gdansk University of Technology, Narutowicza 11/12, 80-233 Gdansk, Poland*
[2]*IMS Laboratory, University of Bordeaux, CNRS UMR 5218, ENSCBP, 16 Av. Pey Berland, 33607 Pessac, France*
[3]*Centre for Plasma and Laser Engineering, The Szewalski Institute of Fluid-Flow Machinery, Polish Academy of Science, Fiszera 14, 80-231 Gdansk, Poland*
[4]*University of Bordeaux, ISM, UMR 5255, F-33400 Talence, France and CNRS, ISM, UMR 5255, F-33400 Talence, France*

(Received 8 October 2012; accepted 27 November 2012; published online 26 December 2012)

Inverted bulk-heterojunction polymer solar cells have been fabricated applying non-metal doped TiO_2 as electron extraction buffer layers. Spin-coated films from nitrogen, sulphur, and iodine doped TiO_2 nanoparticles dispersed in dimethyl sulphoxide showed comparable roughness and uniformity as those from the pure TiO_2 nanoparticles. The highest power conversion efficiency (PCE) of 1.67% was obtained for N-doped TiO_2, whereas in the case of pure TiO_2, PCE was around 1%. The highest short circuit current density ($J_{sc} = 10.66\,mA\,cm^{-2}$) was achieved for I-doped TiO_2. Moreover, it was observed that devices with doped TiO_2 exhibit better stability under constant illumination comparing to the control devices with pure TiO_2. © *2012 American Institute of Physics*. [http://dx.doi.org/10.1063/1.4770490]

I. INTRODUCTION

In recent years, there have been impressive progresses in the performance of organic solar cells with the applications of novel materials or device structures.[1,2] Generally, conventional device architecture includes poly(3,4-ethylenedioxythiophene) doped with poly(styrenesulfonate) (PEDOT:PSS) as hole transport layer and aluminum as electron collecting electrode, both of which are sensitive to water and oxygen, thus limiting device stability in ambient condition. An alternative approach is to use an inverted structure where indium tin oxide (ITO) acts as electron collecting and high work function metals such as Ag and Au as hole collecting electrodes, respectively. Oxide buffer layers (TiO_2, ZnO, MoO_3, etc.) are usually inserted to improve charge extraction either for electrons or holes. In this way, both PEDOT:PSS and Al can be discarded, which result in better long term stability and efficiency.[3] A thoughtful control over these interfaces could enhance the performance of the devices significantly. A few examples are: the deposition of self-assembly monolayer on the titania surface;[4] control of the morphology of titania layer (i.e., nanotubes[5]); and direct modification of the electronic structure by doping.[6]

Metal doped titania with Mn or Nb atoms were proposed for application in inverted organic photovoltaic cells. Aplarslan *et al.*[7] reported buffer layers of Mn-doped TiO_2 with different contents of dopant atoms using P3HT: PCBM as active layer. Despite higher absorbance of Mn-TiO_2 layers, the solar cells' efficiency with doped titania increased by 38% in comparison to layer without Mn-dopant. The inverted solar cells with Nb-doped titania were proposed by Lira-Cantu *et al.*,[8,9] using MEH-PPV (Poly[2-methoxy-5-(2-ethylhexyloxy)-1,4-phenylenevinylene]) as an active layer. In the case of 20% atomic content of Nb, the efficiency reached 0.074% (for pure titania layer, power conversion efficiency (PCE) was 0.042%). Both studies showed better stability of the devices for doped titania as a buffer layer.

Until now, no study has been reported for non-metal doped titania for inverted organic solar cells. However, non-metal doped titanium dioxides have been successfully applied in dye sensitized solar cells. Strong effects were observed in the efficiencies of these types of cells, when iodine doped,[10] nitrogen doped,[11,12] and nitrogen and sulphur co-doped titania[13] were compared to pure TiO_2. In these systems, occurrence of dopant atoms was responsible for higher absorption of visible light, a higher rate of dye adsorption and recombination retardation.[14]

In this paper, we present our studies concerning the replacement of pure titanium dioxide by non-metal (sulphur, nitrogen, iodine) doped titania in inverted organic solar cell devices with the aim to control the interface between the active layer and ITO for efficient charge collection. Film morphology, solar cell parameters, and device stability were compared to the control devices based on pure TiO_2.

II. EXPERIMENTAL

Commercially available regioregular Poly(3-hexylthiophene-2,5-diyl) (P3HT) (Plextronics) and Phenyl-C61-butyric acid methyl ester (PCBM) (>99.5%, Solaris) have been used without further purification. Organic solar cells were prepared according to the following procedure: ITO-coated glass electrodes (10 Ω/sq, Kintec Company) were partially etched followed by ultrasonic cleaning in successive solutions of de-ionized water, acetone, ethanol, and isopropanol. In each solvent, substrates were immersed for 15 min. Then, the ITO substrates were subjected to UV-ozone treatment in order to increase the hydrophilic nature

a)E-mail: mamatimin.abbas@ims-bordeaux.fr.

of the surface and to remove any residual organic contamination. Different doped titania were obtained on the basis of original synthesis methods. Preparation methods were described in detail in previous works.[15–19] Doping concentrations are 1.21%, 1.21%, and 3.21%, respectively, for N-, S-, and I-doped titania evidenced from XPS studies. Doped and pure titania dispersion (5 mg/ml) in dimethyl sulphoxide (DMSO) (FLUKA) were spin coated on ITO sheets (5000 rpm, 60 s), followed by thermal treatment under vacuum (10 mbar) at 100 °C for 10 min to remove any residual solvent. Active layers were deposited from a 20 mg/ml concentrated solution of P3HT:PCBM (1:1) in 1,2-dichlorobenzene. The layers were cast by spin-coating at 1000 rpm for 25 s. After deposition, the layers were dried in the nitrogen glove box and the trace solvent underwent slow evaporation (solvent annealing). Finally, a 10 nm-thick molybdenum oxide and then a 100 nm-thick silver electrode were thermally evaporated under vacuum (10^{-6} mbar) through a shadow mask determining the active surface area of 10 mm^2.

The thicknesses of titania layers were estimated on the basis of ellipsometry measurement performed using an imaging null-ellipsometer EP3 (Nanofilm). The instrument was used in total internal reflection mode and both the intensity and the phase changes of the reflected light were monitored and converted into two ellipsometric angles Ψ and Δ. Spectroscopic ellipsometry data were recorded at constant angle of incidence (AOI = 55°) and different wavelengths ($\lambda = 360$–900 nm). Contrast ellipsometry images were recorded at AOI = 55° and $\lambda = 658$ nm. Each titania layer was measured twice at different regions of interest (ROIs) with spatial resolution of 2 μm. The data collected from 300 μm × 300 μm areas were evaluated by EP3View V235 software (Nanofilm). For modeling, EP4Model 1.0.1 software (Nanofilm) was used. All the titania films had very similar thickness varying from 96 to 109 nm. The thickness of the active layer measured using profilometer Alfa Tencor was 175 ± 10 nm. Optical absorption of titania and P3HT:PCBM deposited onto titania layers has been investigated using UV-vis spectroscopy. Spectra were recorded over the spectral range of 300-800 nm using a SAFAS UVMC^2 spectrometer on samples spin coated on ITO/glass substrates. Atomic force microscopy has been performed under ambient conditions using a commercial optical deflection microscope (stand-alone configuration for a large sample, AFM VEECO *DI*-3100 with a Nanoscope IIIa, Digital Instrument). Current density-voltage (*J-V*) characteristics of devices were examined using a Keithley 4200 semiconductor analyzer under illumination of an AM1.5 solar simulator set at 100 mWcm^{-2}, which was calibrated using an *IL1*400*BL* radiometer. Samples were measured in dry nitrogen glovebox. The stability measurements were performed under continuous illumination. The current density-voltage characteristics were measured at every 2 min, 5 min, and after 20 min of illumination, until clear decrease in the solar cell parameters was observed.

III. RESULTS AND DISCUSSION

In Fig. 1, the energy diagram and the device structure of the solar cell are presented. Energy levels were referenced to the vacuum level. Special note should be given to very deep ionization energy of the MoO_3, which was revealed in recent studies.[20,21] The value of conduction band energy for each titania was determined using impedance spectroscopy and Mott-Schottky analysis with respect to the assumption that flatband potential is very close to the energy value of conduction band.[22] The position of each valence band was estimated taking into the account the band gap energy value. The detailed description of the band gap energy determination, impedance measurements, and their interpretation was given in the previous works.[15–17] The pure and doped titania materials are characterized by different positions of conduction and valence bands. The positions of the conduction band of all the doped titania are located below the conduction band energy of pure titania. Additionally, the iodine, nitrogen, and sulphur doped titania have narrower band gap energies (2.98 eV for N-TiO_2, 2.93 eV for S-TiO_2, and 2.80 eV for I-TiO_2) than pure TiO_2. Doping of the titania with various dopants introduces additional electronic states in the gap of titania, which was evidenced by the electronic structure study of different dopants in the titania.[23]

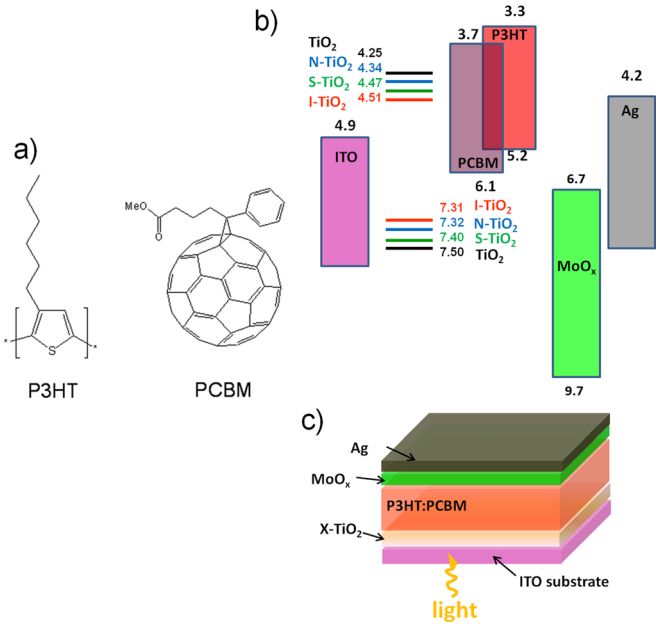

FIG. 1. (a) Chemical structure of P3HT and PCBM; (b) scheme of the energy levels of the materials with respect to the vacuum level involved in the inverted solar cells; (c) photovoltaic device structure in the inverted arrangement used in this work.

The absorption spectra of the ITO/x-TiO_2/P3HT:PCBM films are shown in Fig. 2. As titania thin layers are semi-transparent, the main contributions for the spectra come from the active layer and there are no significant differences between each spectrum. However, slightly stronger absorbance was observed for active layers deposited onto N-TiO_2 and I-TiO_2 buffer layers. It should be noted that the feature at around 600 nm, which comes from π-π interchain interactions between P3HT chains, is rather strong and similar to all the films, confirming optimized active layers through solvent annealing process. Moreover, the observation excludes any influence of the different buffer layers on the P3HT:PCBM

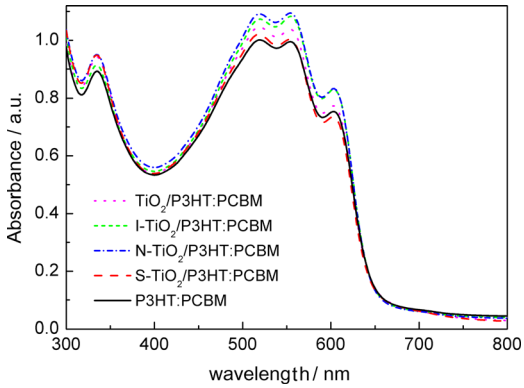

FIG. 2. Absorption spectra of P3HT:PCBM films deposited on different titania layers.

organization, which could play a role in the final device performances.

In Fig. 3, AFM images of pure and doped titania films are displayed. Despite the fact that the layers were deposited from the dispersion of nanoparticles, the morphologies of obtained films are rather satisfactory. All the deposited layers are quite uniform and their root mean square roughnesses vary from 3.33 to 4.47 nm. Film from pure TiO_2 exhibits a slightly higher roughness, which can be due to stronger aggregation of the nanoparticles comparing to the doped ones. A reasonable explanation could be that the doped nanoparticles have surface groups that could facilitate the interaction of the nanoparticles with the polar solvent. Repulsion force between the particles due to the presence of surface groups could also inhibit stronger aggregation in doped titania nanoparticles comparing to undoped ones.

Larger areas of different titania layers were investigated using ellipsometry contrast images as shown in Fig. 4. Although major parts of the film morphologies are comparable for different films, much larger and more distributed

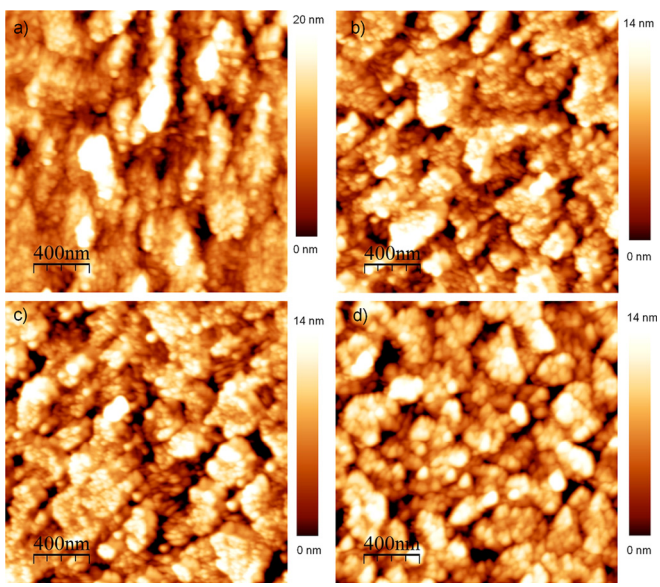

FIG. 3. AFM images of the surfaces of (a) TiO_2 (RMS = 4.47 nm); (b) N-TiO_2 (RMS = 3.36 nm); (c) S-TiO_2 (RMS = 3.33 nm); (d) I-TiO_2 (RMS = 3.37 nm) thin layers spin coated onto ITO substrate from a 5 mg/ml dispersion in DMSO.

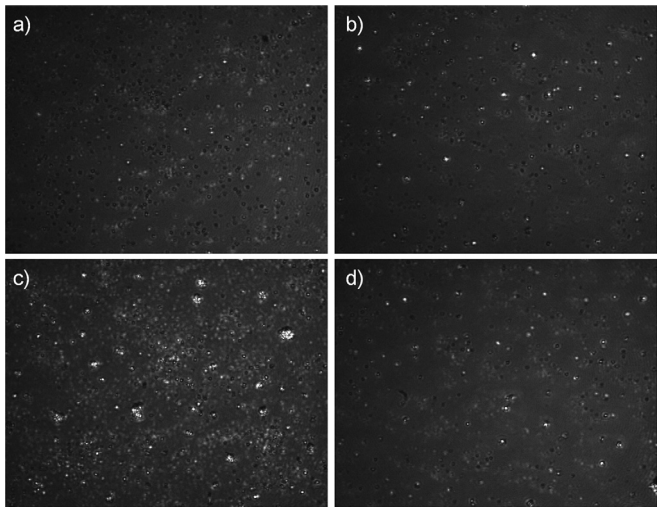

FIG. 4. Ellipsometry contrast images (526 μm × 392 μm) of (a) pure TiO_2, (b) N-TiO_2, (c) S-TiO_2, (d) I-TiO_2 layers deposited onto ITO substrate.

agglomerates were evidenced in the case of S-TiO_2 layer, which came from relatively poor dispersion of S-TiO_2 in DMSO.

In Fig. 5, the solar cell performance parameters (Jsc, Voc, FF, and PCE) for the devices with and without titania layer under continuous illumination are displayed as a function of time. At the beginning of the measurements (up to 20 min), gradual increase in short-circuit current and open circuit voltage was observed. Such light soaking effect took place also in case of the titania free devices, suggesting this effect originates from the interface between the active layer and the MoO_3, probably due to the enrichment of the P3HT phase at this interface following light soaking, as suggested by the work of Wang *et al.*[24] Nevertheless, the effect of dopants manifests during further illumination. For the device with pure titania layer, a clear decrease in the device parameters is observed after about 30 min of illumination and further measurements were stopped after 55 min. In the case of doped titania, a higher stability is noticed even for device with S-doped titania layer, which exhibits lower efficiency than that of pure TiO_2. Probably the dopant atoms act as electron traps. Once the traps are filled by negative carriers, electrons can easily transfer to the ITO contact,[7] thus gradually increasing the solar cell performance. For the device including an N-doped titania layer, a progressive increase in the efficiency during the whole irradiation time was observed.

Apart from the changes in the electronic structure, doped materials can also modify the surface in comparison to pure titania. On the basis of Fourier Transform Infrared Attenuated Total Reflectance (FTIR ATR) spectra presented in the former publications,[16–19] the presence of N-Ti-O and N-H species in N-doped TiO_2 and S = O, S-O, SO_4^{2-} in S-doped TiO_2 powder was observed. The researches devoted to the interface modification between titania and P3HT layer showed that certain groups could strongly affect the performance of solar cells.[25] The surface species could act as mediators of charge transfer between the polymer and the titania layer. Furthermore, the crystalline phases of pure and iodine doped titania were anatase, whereas in the XRD pattern for sulphur doped TiO_2, apart from the anatase signals, small

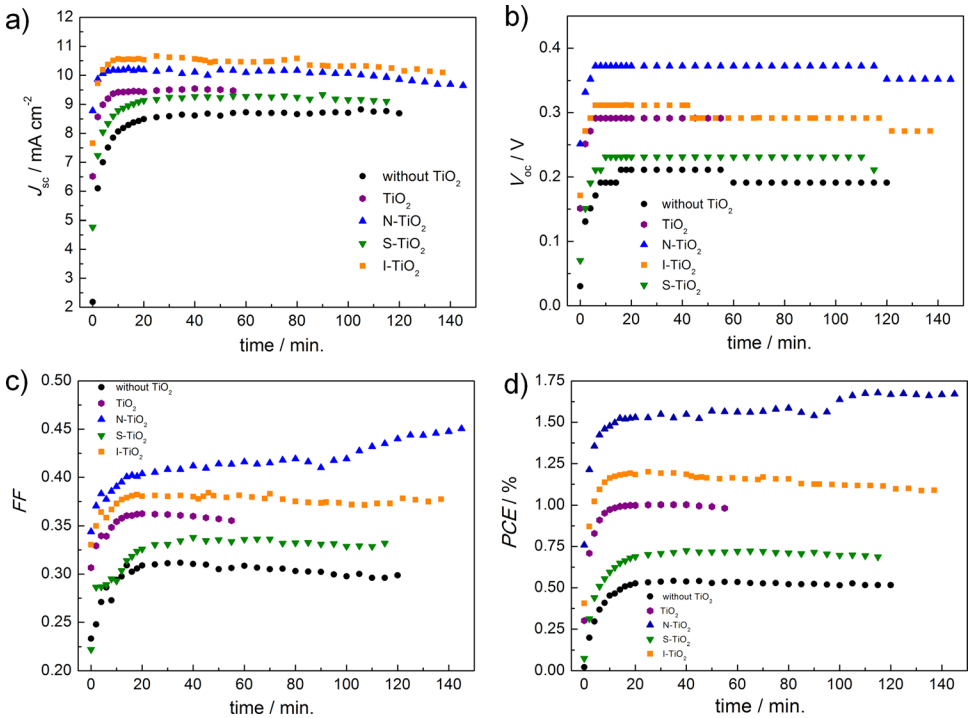

FIG. 5. Stability test under continuous illumination (100 mW cm^{-2}) for inverted solar cells with different titania layers. The changes in terms of solar cell parameters: (a) short-circuit current density, (b) open circuit voltage, (c) fill factor, (d) power-conversion efficiency are shown.

rutile peak was also present. In the case of nitrogen doped titania, the crystalline phase was a mixture of anatase, rutile, and amorphous phases.[19] According to Kang *et al.*,[26] the solar cell with titania buffer layer possessing the amorphous phase exhibited a continuous increase in the performance and it was attributed to the filling up of shallow traps within the amorphous phase during irradiation. Besides, the presence of rutile also plays a role and the increase was observed in current and open circuit voltage for devices with titania layer where the rutile crystalline phase appeared.[8]

Another reason which could affect the device performance upon long term illumination may be the presence of dopants in the lattice structure. The layers of non-stoichiometric TiO_x structure (i.e., obtained by introduction of dopants) are known to show a stronger variation of the work function under irradiation than pure stoichiometric titania.[27] During illumination, O_2^- surface species could be neutralized and consequently oxygen desorption could take place, which causes lowering of barrier for electron extraction leading to the observed increase in fill factor.

Current density-voltage curves of the devices with different titania layers as well as without titania buffer layer are given in Fig. 6. Here, the results are shown when the device performances were stabilized (at the time when the maximum PCE was reached). The associated photovoltaic characteristics are displayed in Table I. All the tested devices with buffer titania layer exhibited better performances than solar cells in which the active layer was directly deposited on ITO. This highlights that the presence of an electron extraction layer helps to improve device efficiencies

Devices based on S-TiO_2 showed slightly lower efficiencies in comparison to pure titania due to poor morphological quality of the film as evidenced in microscopic images. However, V_{oc} and J_{sc} are higher for iodine and nitrogen doped TiO_2. Devices with I-doped TiO_2 reached the highest current density, whereas the maximum V_{oc} and efficiency were obtained for the devices with N-doped TiO_2. Values of each parameter are provided in Table I. The increase in PCE for iodine and nitrogen doped titania in comparison to pure titania layer equals to 20% and 67%, respectively.

We suggest that when a morphological effect is excluded (as in the case of S-TiO_2), doping of titania buffer layer

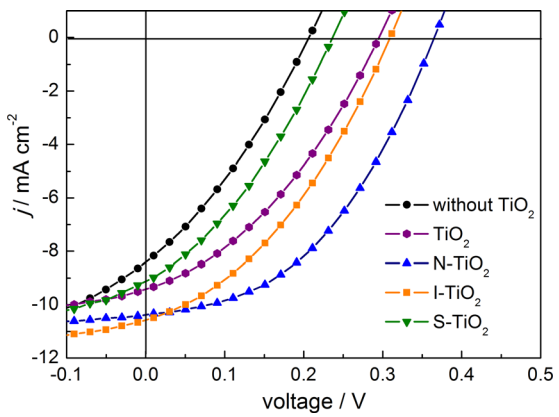

FIG. 6. The current density-voltage (J-V) characteristics of inverted ITO/x-TiO_2/P3HT:PCBM/MoO_x/Ag solar cells with different titania layers.

TABLE I. Device performance parameters for inverted solar cells with the structure: ITO/x-TiO_2/P3HT:PCBM/MoO_x/Ag.

Titania layer	J_{SC} (mA cm^{-2})	V_{oc} (V)	FF	PCE (%)
Without TiO_2	8.59	0.21	0.30	0.54
TiO_2	9.51	0.29	0.36	1.00
N-TiO_2	10.09	0.35	0.47	1.67
S-TiO_2	9.27	0.23	0.34	0.73
I-TiO_2	10.66	0.31	0.36	1.20

optimizes the interface between the active layer and ITO, mainly through the mechanism of better energy level alignment for charge extraction or enhanced charge transport within the layer itself. Better device stability under continuous illumination of the devices with doped titania can be attributed to charge trapping at the intrinsic dopant sites or to the presence of an amorphous or a rutile phase.

IV. CONCLUSIONS

In this work, we studied the effect of different non-metal doped titania buffer layers on the performance of inverted polymer solar cells. Non-metal doped titania layers were successfully adapted to inverted polymer solar cells for the first time. The effect of doping on device properties was clearly visible. Light soaking effect was observed and quite stable performances after about 10 min of illumination were achieved. Among all tested materials, nitrogen doped TiO_2 exhibits the highest efficiency (1.67%) and stability under continuous illumination for 150 min. The increase in PCE for iodine and nitrogen doped titania with respect to pure titania layer is 20% and 67%, respectively. Our results show that when the buffer layer morphologies are comparable, doping of the buffer layer in the inverted polymer solar cells plays significant role in enhancing device performances as well as stability under continuous illumination. Device efficiency could be further increased by optimizing the morphology of the layers using doped precursors rather than nanoparticles or other alternative oxides (such as ZnO).

ACKNOWLEDGMENTS

Financial support from Polish Ministry of Sciences and Higher Education (Grant No. NN209 254238) and from the project The development of interdisciplinary doctoral studies at the Gdansk University of Technology in modern technologies (Project No. POKL.04.01.01-00-368/09) is gratefully acknowledged; M. A. thanks financial support from GIS ADVANCED MATERIALS IN AQUITAINE-CELLORGAFLEX program.

[1]C. J. Brabec, S. Gowrisanker, J. J. M. Halls, D. Laird, S. Jia, and S. P. Williams, Adv. Mater. **22**, 3839 (2010).
[2]M. Helgesen, R. Søndergaard, and F. C. Krebs, J. Mater. Chem. **20**, 36 (2010).
[3]D. H. Wang, D. G. Choi, K.-J. Lee, O. O. Park, and J. H. Park, Org. Electron. **11**, 599 (2010).
[4]S. K. Hau, H.-L. Yip, O. Acton, N. S. Baek, H. Ma, and A. K. Y. Jen, J. Mater. Chem. **18**, 5113 (2008).
[5]B. Y. Yu, A. Tsai, S. P. Tsai, K. T. Wong, Y. Yang, C. W. Chu, and J. J. Shyue, Nanotechnology **19**, 255202 (2008).
[6]X. Fan, G. Fang, S. Guo, N. Liu, H. Gao, P. Qin, S. Li, H. Long, Q. Zheng, and X. Zhao, Nanoscale Res. Lett. **6**, 546 (2011).
[7]Z. Alparslan, A. Ksemen, O. Örnek, Y. Yerli, and S. E. San, Int. J. Photoenergy **2011**, 734618.
[8]M. Lira-Cantu, A. Chafiq, J. Faissat, I. Gonzalez-Valls, and Y. Yu, Sol. Energy Mater. Sol. Cells **95**, 1362 (2011).
[9]M. Lira-Cantu, M. Khoda Siddiki, D. Muñoz-Rojas, R. Amade, and N. I. González-Pech, Sol. Energy Mater. Sol. Cells **94**, 1227 (2010).
[10]Q. Hou, Y. Zheng, J. F. Chen, W. Zhou, J. Deng, and X. Tao, J. Mater. Chem. **21**, 3877 (2011).
[11]W. Guo, L. Wu, Z. Chen, G. Boschloo, A. Hagfeldt, and T. Ma, J. Photochem. Photobiol., A **219**, 180 (2011).
[12]H. Tian, L. Hu, C. Zhang, W. Liu, Y. Huang, L. Mo, L. Guo, J. Sheng, and S. Dai, J. Phys. Chem. C **114**, 1627 (2010).
[13]K. Prabakar, M.-k. Son, D. Ludeman, and H.-j. Kim, Thin Solid Films **519**, 894 (2010).
[14]T. Ma, M. Akiyama, E. Abe, and I. Imai, Nano Lett. **5**, 2543 (2005).
[15]K. Szybowska and A. Lisowska-Oleksiak, Solid State Ionics **188**, 165 (2011).
[16]K. Siuzdak and A. Lisowska-Oleksiak, in *18th International Conference on Solid State Ionics Warsaw, Poland*, 2011, p. 283.
[17]K. Siuzdak, "Synthesis and characterization of non-metal atom doped titanium dioxide as electrode material active under visible light illumination," Ph.D. dissertation (Gdansk University of Technology, 2012).
[18]A. Lisowska-Oleksiak, K. Szybowska, and V. Jasulaitiené, Electrochim. Acta **55**, 5881 (2010).
[19]K. Szybowska, M. Gazda, and A. Lisowska-Oleksiak, Adv. Mater. Sci. **9**, 23 (2009).
[20]M. Kröger, S. Hamwi, J. Meyer, T. Riedl, W. Kowalsky, and A. Kahn, Appl. Phys. Lett. **95**, 123301 (2009).
[21]J. Meyer, A. Shu, M. Kröger, and A. Kahn, Appl. Phys. Lett. **96**, 133308 (2010).
[22]J. Y. Kim, D. W. Kim, H. S. Jung, and K. S. Hong, Jpn. J. Appl. Phys., Part 1 **44**, 6148 (2005).
[23]X. Chen and C. Burda, J. Am. Chem. Soc. **130**, 5018 (2008).
[24]J. C. Wang, C. Y. Lu, J. L. Hsu, M. K. Lee, Y. R. Hong, T. P. Perng, S. F. Horng, and H. F. Meng, J. Mater. Chem. **21**, 5723 (2011).
[25]C. Goh, S. R. Scully, and M. D. McGehee, J. Appl. Phys. **101**, 114503 (2007).
[26]Y. J. Kang, C. Su Kim, D. Sung You, S. Hoon Jung, K. Lim, D. G. Kim, J. K. Kim, S. Hyung Kim, Y. R. Shin, S. H. Kwon, and J. W. Kang, Appl. Phys. Lett. **99**, 073308 (2011).
[27]H. Schmidt, K. Zilberberg, S. Schmale, H. Flügge, T. Riedl, and W. Kowalsky, Appl. Phys. Lett. **96**, 243305 (2010).